

Automated Detection of Z-Axis Coverage with Abdomen-Pelvis Computed Tomography Examinations

Min Zhang · Clinton Wellnitz · Can Cui ·
William Pavlicek · Teresa Wu

Published online: 21 November 2014
© Society for Imaging Informatics in Medicine 2014

Abstract Excessive cephalocaudal anatomic (Z-axis) coverage can lead to unnecessary radiation exposure to a patient. In this study, an automated computing model was developed for identifying instances of potentially excessive Z-axis coverage with abdomen-pelvis examinations. Eight patient and imaging attributes including patient gender, age, height, weight, volume CT dose index (CTDI_{vol}), dose length product (DLP), maximum abdomen width, and maximum abdomen thickness were used to build a feedforward neural network model to predict a target Z-axis coverage whether it is an excessive or non-excessive Z-axis coverage scans. 264 CT abdomen-pelvis exams were used to develop the model which is validated using 10-fold cross validation. The result showed that 244 out of 264 exams (92.4 %) correctly predicted Z-axis excessive coverage. The promising results indicate that this tool has the potential to be used for CT exams of the chest and colon, urography, and other site-specified CT studies having defined limited length.

Keywords CT dose · Z-axis coverage · Monitoring · Feature analysis · Neural network · Quality control

Background

Computer-aided tomography (CT) is undergoing an intensive refinement of x-ray radiation dose administration controls with the goal of markedly lowering the patient dose [1]. A

number of advanced technologies and practice changes are now used to lower radiation dose with CT, such as automatic tube current modulation (ATCM) [2], a variety of de-noising techniques enabling reduced patient exposure [3], reducing kVp for smaller patient size [4], and reducing the number of contrast phase acquisitions [5]. One additional source of potential unnecessary exposure to a patient can occur due to excessive Z-axis coverage. Z-axis coverage (extent of CT x-ray exposure to the patient in the cephalocaudal direction) primarily depends upon the patient size and the specific exam being performed (i.e., the CT protocol). For the abdomen-pelvis exam, the most frequently encountered body CT use, it also depends on (1) the movement of the diaphragm during breathing, (2) the possibility of actual patient movement on the table, (3) the need to always fully include all the required anatomy, and (4) the CT scanner software controls for refinement of the extent of Z-axis coverage (indicated by the defined scan range) in comparison to the actual radiation-exposed anatomy (overscan compensation). Some clinical sites standardize the anatomical features to be selected by the technologists when positioning the defined scan range acquisition box. Technologists recognize any “missed anatomy” results in the need to acquire a second acquisition—thereby causing added (overlapped) exposure to the patient and a second acquisition to be merged with the CT exam for interpretation. A second scan to acquire a few added centimeters of anatomy not only results in overlapped radiation being given to “imaged” tissue but also includes added overlapped radiation due to “overscan”—the term used to make note that the radiation field is larger than the Z-axis detector coverage in order to fully expose the detectors. As a result, to be fully confident that complete coverage occurs the first time, it is possible that an overly generous setting of defined scan range is chosen—one which may well result in greater Z-axis coverage than is needed. Some recent studies note that as much as 98 % of body CT scans exceeds the predefined anatomic boundaries of

M. Zhang · C. Cui · T. Wu
School of Computing, Informatics Decisions and System
Engineering, Arizona State University, Tempe, AZ, USA

M. Zhang · C. Wellnitz · W. Pavlicek (✉)
Department of Radiology, Mayo Clinic, 13400 E. Shea Boulevard,
Scottsdale, AZ 85259, USA
e-mail: pavlicek.william@mayo.edu

their respective scan protocols [2, 6]. Therefore, a method that is able to automatically detect excessive Z-axis coverage may provide a helpful quality assurance (QA) tool for potentially reducing this source of unnecessary patient exposure.

Methods

Excessive Z-Axis Coverage

There is no agreement or standardized definition of excessive Z-axis coverage of CT exam in the literature for the routine abdomen-pelvis examination. A reason for this may be that this type of exam is a breath hold acquisition, so inpatients or respiratory-compromised patients may be found to have generous Z-axis coverage that is appropriate due to their condition. Based on a sample of the normal variation observed with the *outpatient* population by the radiologists in our hospital, 2 cm was chosen to determine the acceptable start and stop positions. To aid in the specification of appropriate versus excessive Z-axis coverage, Z-axis coverage for the abdomen-pelvis CT examination are defined as follows:

- “Ideal” start position The location of the superior most aspect of left or right hemidiaphragm, whichever is most superior (red circled in Fig. 1).
- Acceptable start position A location less than or equal to 2 cm superior to the location of the superior most aspect of the left or right hemidiaphragm. The technologists

ideally start scanning no more than 1 cm superior to the ideal start position, but it is acceptable to start up to 2 cm.

- Threshold of excessive start position A location greater than 2 cm superior to the location of the superior most aspect of the left or right hemidiaphragm, whichever is more superior.
- Ideal stop position The location of the inferior most aspect of left or right ischial tuberosity, whichever is more inferior (red circled in Fig. 2).
- Acceptable stop position A location less than or equal to 2 cm inferior to the location of the inferior most aspect of the left or right ischial tuberosity, whichever is more inferior.
- Threshold excessive stop position A location greater than 2 cm inferior to the location of the inferior most aspect of the left or right ischial tuberosity, whichever is more inferior.
- Ideal Z-axis coverage A scan length equal to the absolute value of the difference between the ideal start and stop positions as shown in Fig. 3a. (A Z-axis coverage may be ideal per this definition, but the start and stop positions may not.)
- Acceptable Z-axis coverage A scan length less than or equal to the absolute value of the difference between the acceptable start and stop

“Ideal” Start Position

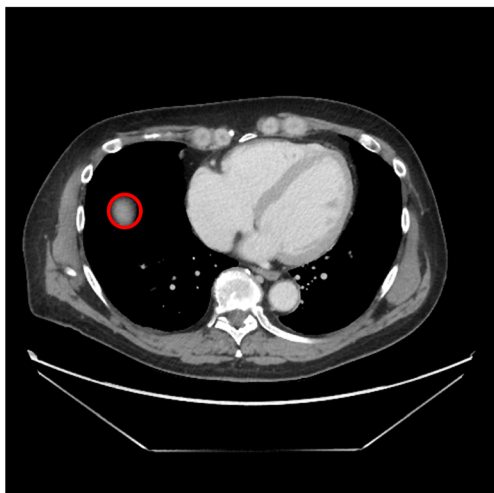


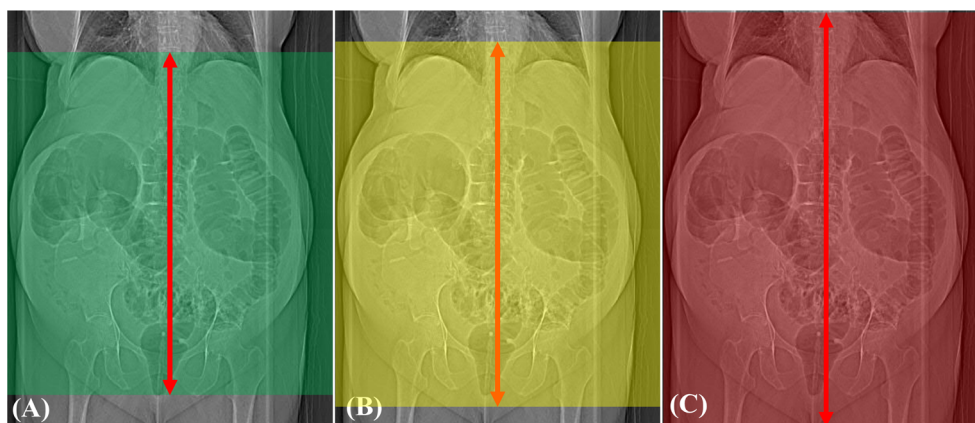
Fig. 1 Ideal start position of CT abdominal scan. Slice location of first image with subdiaphragmatic tissue (*left or right*) is defined as ideal start position of CT scan

“Ideal” Stop Position



Fig. 2 Ideal stop position of CT abdominal scan. Slice location of last image with ischial tuberosity bone (*left or right*) is defined as ideal stop position of CT abdominal scan

Fig. 3 Different situations of Z-axis coverages. *Transparent boxes* are the defined scan ranges for Z-axis coverage. **a** Ideal Z-axis coverage. **b** Acceptable Z-axis coverage. **c** Excessive Z-axis coverage



positions but greater than the ideal Z-axis coverage as shown in Fig. 3b. (A Z-axis coverage may be acceptable per this definition, but the start and stop positions may not be.)

Excessive Z-axis coverage

A scan length greater than the absolute value of the difference between the acceptable start and stop positions as shown in Fig. 3c.

In this study, the actual Z-axis coverages are calculated manually as the distance of first axial image slice to the last axial image slice which is based on actual patient CT and anatomical data from picture archiving and communication system (PACS).

For newer CT devices, the actual Z-axis coverage information is provided in enhanced Digital Imaging and Communications in Medicine Structured Report (DICOM SR) object. The start and stop positions are available in the DICOM header (TAG: 0008,0104) of Radiation Dose Structure Report (RDSR) as shown in Table 1. Therefore, the actual Z-axis coverage can be obtained by calculating the distance between the top Z location and the bottom Z location of the scanning length. For those scanners not having RDSR, Z-axis coverage can be either measured manually by PACS or measured automatically by using image processing techniques [13, 14]. At this time, the anatomical landmarks of the patient that correspond to an irradiation event are not available in DICOM and thus no reference to patient coverage can be directly obtained.

Table 1 Z-axis coverage information from new DICOM standard of RDSR

(0008,0104)—Code meaning [LO][34][1]: top Z location of scanning length
(0008,0104)—Code meaning [LO][36][1]: bottom Z location of scanning length

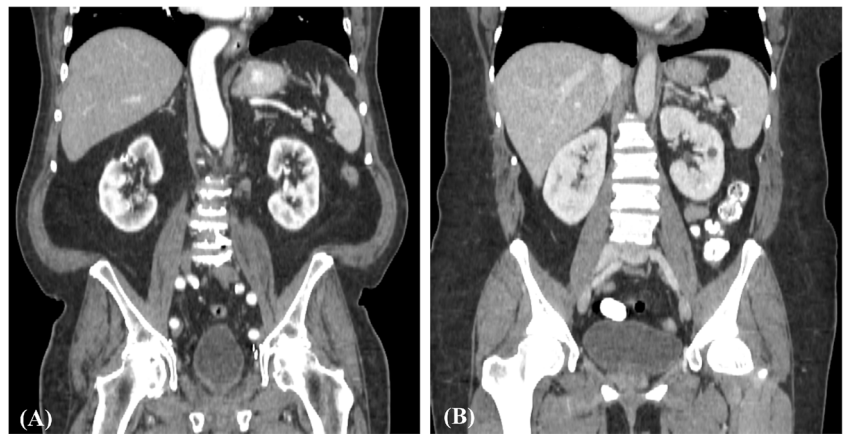
We specify that should our measured Z-axis coverage is greater than and/or equal to ideal Z-axis coverage and less than and/or equal to acceptable Z-axis coverage, it is not excessive Z-axis coverage. Greater values of coverage are defined as excessive Z-axis coverage and should be detectable when using a QA tool. The real patient examples are shown in Fig. 4.

Data Collection and Features Selection

This institutional review board and HIPAA compliant study included 264 patients having routine abdominal studies between year 2012 and year 2014. The age of the patients in this study ranges from 19 to 93 and the gender distribution includes 140 females and 124 males.

In abdominal exams, six patient physical features, including age, gender, height, weight, lateral-anteroposterior abdominal dimension (thickness), and posteroanterior-mediolateral abdominal dimension (width) of the patient, and two radiation dose features, volume CT dose index (CTDIvol) and dose length product (DLP), were used. As a result, eight features can be collected for the predictive model development. DICOM Index Tracker (DIT) [7] was used to obtain patient gender, age, height, weight, CTDIvol, and DLP data. GE Centricity (our PACS) provided values of maximum abdominal width and maximum abdominal thickness information as individually measured using a measurement tool. Examples of these measurements are given in Figs. 5 and 6. Note that our use of patient “width” as a feature for the statistical approach may be a source of error as this measurement is computed for a plane at isocenter, while a patient’s projected image size depends upon the source to object distance and may differ from isocenter. Here we used the measured width as an estimation to approximate the real abdominal width of the patient in developing the model. It is our

Fig. 4 Real patient Z-axis coverages. **a** Not excessive Z-axis coverage. **b** Excessive Z-axis coverage



intention to study the impact of the estimation on model performance as a future work.

To validate the model, the ideal Z-axis coverage and acceptable Z-axis coverage were manually measured. Thus those exams found having excessive Z-axis coverage were formally identified for model building and training purposes.

Imbalanced Data Resampling

In this study, among 264 cases, it is observed that 237 out of 264 patients do not have excessive Z-axis coverage resulting in the dataset being imbalanced. When imbalanced data sets are presented, most data learning algorithms may fail to provide favorable accuracies to determine the classes (e.g., excessive Z-axis coverage vs. non-excessive Z-axis coverage) and the data [8]. To handle the imbalanced classification, a statistically appropriate way is to use resampling methodology in which data from the minority class is randomly repeated

and oversampled while the data from majority class is randomly eliminated and downsampled. This results in the number of instances from minority class being reasonably similar to the number of instances from majority class. After resampling process, the class distribution is balanced and uniformed.

Feedforward Neural Networks

Artificial neural network (ANN) model simulates biological neural networks of human brain for decision-making (supervised learning algorithm) as a type of supervised learning. The type of ANN used in this study was feedforward neural network with back-propagation learning algorithm [9]. Feedforward neural network is composed of three different layers: input layer, hidden layers, and output layer, and there is no feedback between layers (thus “feedforward”). The input layer is formed of attributes of input data; the hidden layer extracts important features contained in the input data, while

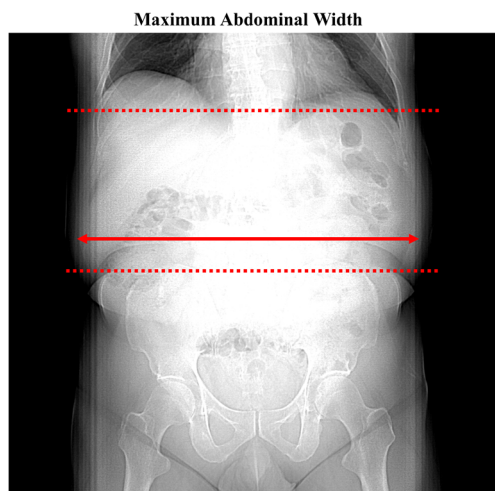


Fig. 5 Maximum abdominal width measurement. Width is measured as the widest skin to skin horizontal dimension below the diaphragm but above the iliac crests

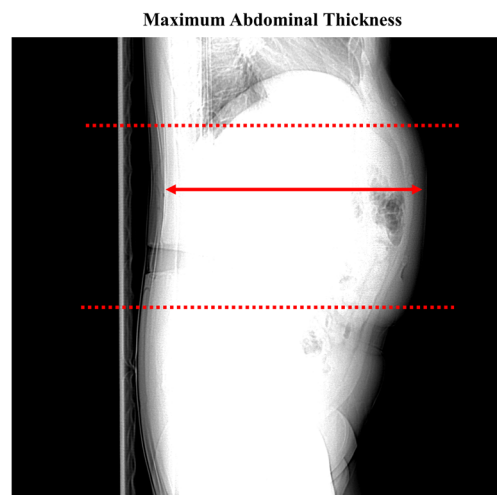


Fig. 6 Maximum abdominal thickness measurement. Thickness is measured as the thickest skin to skin horizontal dimension below the diaphragm but above the iliac crests

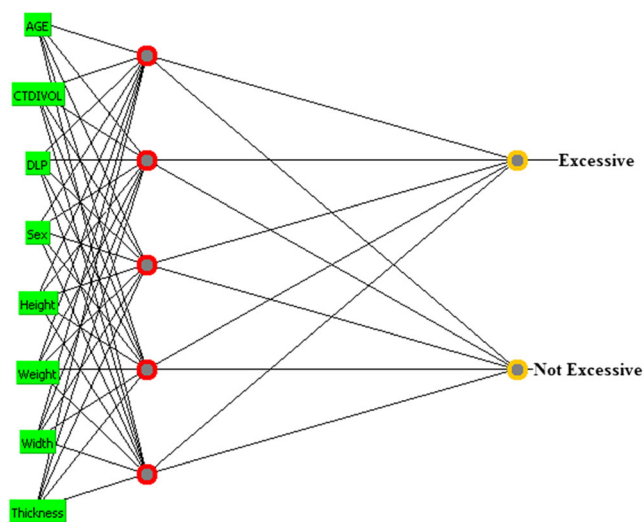


Fig. 7 Diagram of feedforward neural network model with five hidden units and two outputs

the output classes form the output layer. The number of hidden layers and number of hidden units were determined following the rules in [10]. The neural network model in final use is given in Fig. 7.

Experimental Results

First, the eight features of input data were standardized (data was subtracted by their mean and divided by their standard deviation) for the purpose of improvement of model performance. Next, the resampling method was performed as we stated above. After standardization and resampling, 10-fold cross validation was used in which data was equally divided into 10 folds. In each experiment, onefold data was used for testing while the other ninefold data were used as training data. A total of 10 experiments were conducted. Results from each experiment were accumulated and summarized as final result.

The ANN model available from WEKA [10] is used. For the parameter settings of neural networks, the logistic sigmoid function was chosen as transfer function; the learning rate is set to be 0.2, while the momentum is set to be 0.1 after tuning.

The maximum number of epochs is set to 600 when the model is not converging.

As shown in Table 2, true positive rate (TP rate), false positive rate (FP rate), precision, and recall were used as metrics to evaluate the performance of ANN model on the data. For excessive class, the TP rate is 0.942, which means that 94.2 % of true positive excessive Z-axis scanners can be retrieved and identified by our model. That is very important to quality assurance of radiation dose. In our test data set, it shows that 244 instances out of 264 are classified correctly whereas only 20 of them are misclassified. The results show that this model is very promising and 92.42 % of the data was classified correctly.

Discussion

Ideally, a tool that could automate a correct Z-axis coverage for each CT scanner with a minimum of operator interaction would be very helpful. This tool would require some landmarking of the patient on the patient support system. If not available a priori an acquisition, a tool that is accurate and available for use as a background review and process QA of a clinically used CT scanner can provide an opportunity for radiation dose reduction [11, 12]. Its help will be to elevate awareness and improve technologist selection of defined scan range and Z-axis coverage for the abdomen-pelvis CT exam. This approach can be applied to protocol-specific measurement of Z-axis coverage including CT brain exams and CT chest exams which have clearly defined boundaries. However, potential limitations may exist with the ANN predicting Z-axis coverage in pediatric patients, since size is quite variable among pediatric patients. It remains to be seen if the tissue contrast is sufficient to provide actionable results.

In this study, the maximum width and maximum thickness of abdomen were determined manually using the PACS measurement tool. However, this process could be automated by using an image processing technique that includes the consideration of the effect of magnification of the CT radiograph [13, 14]. While eight attributes were used and were shown to be

Table 2 Detection result on 264 CT abdominal exams

Class	TP rate	FP rate	Precision	Recall	F measure	ROC area
Excessive	0.942	0.091	0.898	0.942	0.919	0.905
Not excessive	0.909	0.058	0.949	0.909	0.929	0.905

Correctly classified instances 244 of 264, percentage 92.4242 %. Incorrectly classified instances 20 of 264, percentage 7.5758 %

reasonably predictive of instances of truly excessive (as defined) Z-axis coverage, other feature sets could be used or more could be added to further improve the predictive accuracy.

Conclusion

This study indicates that a model using eight attributes can provide high performance for routine monitoring of Z-axis anatomical coverage with abdomen-pelvis CT exams. An abdomen-pelvis exam identified by this tool as potentially having “excessive” Z-axis coverage is correctly identified about 92.4 % of the time. This quality assurance tool can be used with CT exams of the chest and colon, urography, and other site-specified CT studies having defined limited length.

References

1. Yu L, Liu X, Leng S, Kofler JM, Ramirez-Giraldo JC, Qu M, Christner J, Fletcher JG, McCollough CH: Radiation dose reduction in computed tomography: techniques and future perspective. *Imaging Med* 1:65–84, 2009
2. Kalra MK, Maher MM, Toth TL, Kamath RS, Halpern EF, Saini S: Radiation from “extra” images acquired with abdominal and/or pelvic CT: effect of automatic tube current modulation¹. *Radiology* 232(2):409–414, 2004
3. Manduca A, Yu L, Trzasko JD, Khaylova N, Kofler JM, McCollough CM, Fletcher JG: Projection space denoising with bilateral filtering and CT noise modeling for dose reduction in CT. *Med Phys* 36(11):4911–4919, 2009
4. Szucs-Farkas Z, Verdun FR, von Allmen G, Mini RL, Vock P: Effect of X-ray tube parameters, iodine concentration, and patient size on image quality in pulmonary computed tomography angiography: a chest-phantom-study. *Investig Radiol* 43(6):374–381, 2008
5. Graser A, Johnson TR, Chandarana H, Macari M: Dual energy CT: preliminary observations and potential clinical applications in the abdomen. *Eur Radiol* 19(1):13–23, 2009
6. Liao EA, Quint LE, Goodsitt MM, Francis IR, Khalatbari S, Myles JD: Extra Z-axis coverage at CT imaging resulting in excess radiation dose: frequency, degree and contributory factors. *J Comput Assist Tomogr* 35(1):50, 2011
7. Wang S, Pavlicek W, Roberts CC, Langer SG, Zhang M, Hu M, Morin RL, Schueler BA, Wellnitz CV, Wu T: An automated DICOM database capable of arbitrary data mining (including radiation dose indicators) for quality monitoring. *J Digit Imaging* 24(2):223–233, 2011
8. Haibo H, Garcia EA: Learning from imbalanced data. *IEEE Trans Knowl Data Eng* 21(9):1263–1284, 2009
9. Sandberg IW: Nonlinear dynamical systems: feedforward neural network perspectives. John Wiley & Sons, 2001
10. Hall M, Frank E, Holmes G, Pfahringer B, Reutemann P, Witten IH: The WEKA data mining software: an update. *ACM SIGKDD Explor Newsl* 11(1):10–18, 2009
11. McCollough CH: Automated data mining of exposure information for dose management and patient safety initiatives in medical imaging. *Radiology* 264(2):322–324, 2012
12. Hara AK, Wellnitz CV, Paden RG, Pavlicek W, Sahani DV: Reducing body CT radiation dose: beyond just changing the numbers. *Am J Roentgenol* 201(1):33–40, 2013
13. Ikuta I, Warden GI, Andriole KP, Khorasani R, Sodickson A: Estimating patient dose from X-ray tube output metrics: automated measurement of patient size from CT images enables large-scale size-specific dose estimates. *Radiology* 270(2):472–480, 2014
14. Cheng PM, Vachon LA, Duddalwar VA: Automated pediatric abdominal effective diameter measurements versus age-predicted body size for normalization of CT dose. *J Digit Imaging* 26(6):1151–1155, 2013